Air and Particle Flow in a Drive Enclosure

by

Michael DeBar, Dorian Liepmann, and Omer Savas

Fluid Mechanics Lab,

University of California, Berkeley

Project Summary of work completed from 1/96 through 1/97

Submitted to SyQuest Technologies, Inc.

1 Introduction

1.1 Motivation

As disk drive capacities increase and access times decrease, higher disk rotation rates and lower head flying heights are becoming more common in hard drives. This makes the assembly more sensitive to dust and other particles that may enter the drive enclosure. Unlike sealed hard drives, where the air can be evacuated to reduce contamination, unsealed systems, such as removable hard drives, accumulate contaminants every time a disk is inserted into the drive. Accretion of these contaminants will result in head crashes and the potential for data to be lost or corrupted.

Combating this problem requires an understanding of the transport phenomena within the drive enclosure and the disk cartridge itself. Many of the standard techniques used to measure field variables in flows are too intrusive to be used in drive enclosures. Hot wire anemometry and laser Doppler velocimetry alter the original flow, since the probes used to take these measurements are too large to insert into an unmodified, operating drive. Opening the drive to accommodate these probes introduces a new set of boundary conditions, modifying the original flow beyond recognition. The probes themselves may generate vortical structures that persist for long times, causing changes in the problem being studied. A new set of analytical tools must be assembled to allow more passive measurements of pressures and velocities within the drive itself.

1.2 Project Goals

The primary goal of this research is to develop a method for rapid, accurate analysis of disk drive systems. In addition to the standard technique of flow visualization used to qualitatively assess the nature of the transport phenomena, shear-sensitive liquid crystals can measure shear stresses on the surface of the disk platter.

Although the disk cartridge must be disassembled to apply the liquid crystals to the disk surface, it can be tested under normal operating conditions, maintaining the original boundary conditions imposed by the drive enclosure. The relevant surfaces of the drive and disk hardware must be constructed from an optically clear material to allow observation of the liquid crystals on the disk surface during tests, but if care is taken to duplicate the original geometry, these changes will not affect the flow significantly.

Both flow visualization and liquid crystal stress measurement are easy to execute, once a procedure has been established. The qualitative features of flow visualization validate the data acquired by the shear stress tests, providing a self-consistency check on the results of the liquid crystal data. The shear stress data determines a velocity profile away from the disk surface and reveals quantitative details of transport phenomena within the drive enclosure, including local velocities and pressures. From these results, design modifications can be introduced to decrease entrainment of foreign particles into the drive and their subsequent interactions with the read/write head and media.

1.3 Background

1.3.1 Governing Analytical Principles

The dominant influence on the fluid within the drive enclosure is the spinning platter. The viscous drag of the rotating disk results in an symmetric tangential stress gradients near the disk surface, while centrifugal forces induce radial stress gradients proportional to radial location. This combination of forces near the disk surface induces a flow near the surface that simultaneously rotates with the disk and expands toward the outer radius of the disk. Since there is a

net outward flow from the center to the outside of the disk, a region of low pressure is induced at the center of the disk near its surface. Due to the disparity in pressure between this low pressure region and the higher pressure region higher above the disk, air flows toward the disk surface in the region near the center of the disk. This effect, shown in Figure 1, is known as "von Karman's viscous pump." [Panton, 1984]

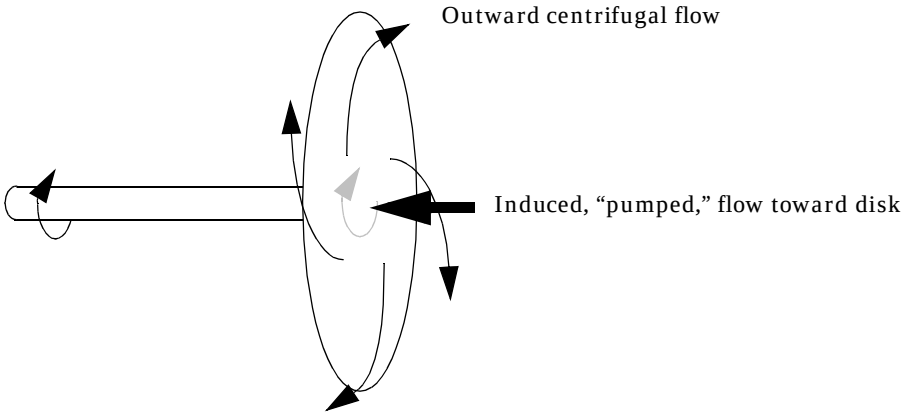

Figure 1: von Karman's Viscous Pump (oblique view)

The maximum Mach number (v/a) for this flow is about 0.1, since the maximum velocity in the flow is about 30 m/s, and the speed of sound in air at STP is 330 m/s. Although this flow can be considered incompressible to within an error of order Ma^2 (~1%), the flow within the drive enclosure differs in several ways from the case of the infinite rotating disk in an incompressible fluid studied by Karman [Karman, 1921] and pictured in Figure 2. The most significant differences are the presence of the reader arm and the sides and top of the disk cartridge. One of the most important features of this problem is the thickness of the boundary layer that forms above the disk surface. According to classical analysis of the infinite disk problem [Karman, 1921], the thickness of the layer δ is approximately $5.4(\nu/\omega)^{1/2}$ = 0.85mm, where δ is defined as the height above the disk at which the tangential velocity drops to 1% of its value on the surface of the disk. In the case of an enclosed disk, this layer should be roughly the same height, since the top of the cartridge provides ample clearance for the boundary layer to form (3 to 4 millimeters). The reader arm and head will also affect the flow. Like any stationary bluff body in a flow, a wake will be associated with the body. The exact effects depend on the velocity of the air before encountering the arm and head, but with the anticipated velocities in the drive, separation should be expected.

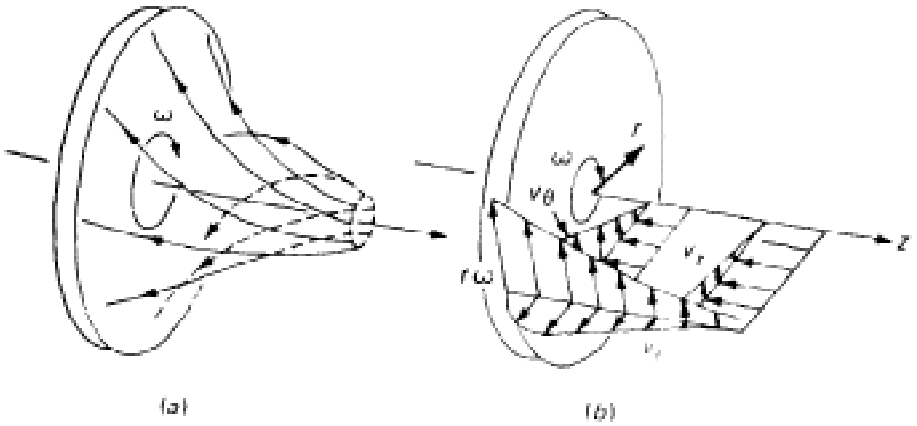

Figure 2: Velocity Profiles on an Infinite Disk:
(a) Streamlines and (b) Velocity components [From White]

While the presence of the side walls of the disk cartridge have effects on the magnitudes of forces, the underlying physical principles are the same. Since the flow is steady and enclosed, a cell-like structure forms within the drive. Centrifugal forces push the air near the disk surface to the outer radius and into the slower-moving regions of the enclosure away from the platter. The region of low pressure near the disk's center draws in higher pressure air from the armature area. This motion takes place near the top and bottom of the drive enclosure, away from the disk surface. Upon reaching the low pressure region, the centrifugal forces exerted by the disk surface push the fluid outward, beginning the cycle again. From an Eulerian point of view, this flow is steady if the flow does not become turbulent.

Kobayashi's research on a spinning disk with no enclosure revealed instability at a critical Reynolds' number (defined as $Re = \omega r^2/\nu$) of about 8.8×10^4 [Kobayashi, et. al., 1980]. Therefore, for a disk spinning in air ($\nu = 1.4 \times 10^{-5}$ at 273K) at 5400 rpm ($\omega = 180\pi$ rad/s) outside of an enclosure, the expected critical radius for the first sign of instability is about 4.7 cm. The onset of the transition to turbulence occurs at about twice this distance, or 9.4 cm. The radius of the platter used in this experiment was about 5 cm, but the changes in boundary conditions must be examined when comparing this radius to Kobayashi's data. The radius of the disk is of the same order as the radius at which instability begins to appear, so some instability might be expected at the outer edges of the disk, depending on interaction with the thin boundary layer that will form on the side walls of the disk cartridge.

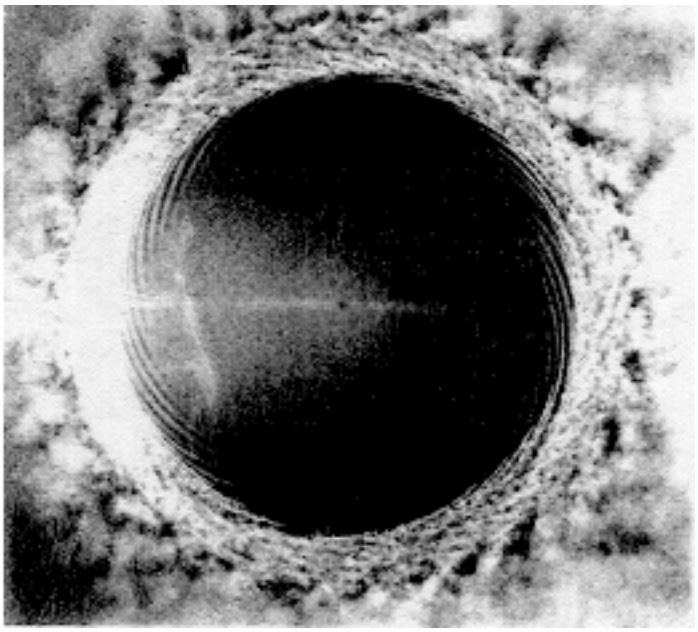

Figure 3: Flow pattern on a disk rotating in air at 1800 rpm. Laminar flow becomes unstable at r = 8 cm, laminar vortices form at r = 12 cm, and transition to turbulence is at r = 16 cm. [From White, after Kobayashi, et. al.]

1.3.2 Flow Visualization

Flow visualization is an essential part of any experiment directed toward the determination of a flow field. Normally, this is accomplished by introducing some type of easily visible particle into the moving flow, and observing its motion. To minimize the deviation of particle velocity from the fluid velocity, the particles should be neutrally buoyant in the surrounding fluid to reduce inertial or buoyancy errors and the particles should be small to reduce drag effects. A natural choice for air flows is smoke, which can be generated in the lab by burning oils, wood,

or even cigarettes [Merzkirch, 1987].

The introduction of these types of particles into a hard drive results in a greater concentration of potentially destructive contaminants into the system, and may leave a viscous residue within the drive upon cooling. An alternative to creating smoke by combustion is generating a fog of frozen water vapor by supercooling air until droplets of water vapor condense and freeze. When the temperature of the fog rises, the frozen droplets melt and condense on surfaces. In the disk drive, water would condense on the sides and top of the drive, and on the platter. Although the presence of water within the drive can damage it, the drive can be shut down if water begins to accumulate. After the water has evaporated from inside the drive, experiments can be resumed. If distilled water is used, little residue will remain after the evaporation process.

Frozen water vapor is not the ideal choice for this experiment, since the lower temperature of the air may induce buoyancy effects into the system; however, buoyancy forces are negligible in the regions of interest of this study, as the velocities in the horizontal plane are much larger than any buoyancy-induced vertical velocities. In addition, upon mixing with room temperature air, frozen vapor particles melt, becoming invisible after relatively short times (on the order of the time required for the disk to make one revolution).

1.3.3 Liquid Crystals

While flow visualization paints a qualitative picture of the fluid flow within a given system, the magnitudes of velocities in the system can only be estimated. In cases where more specific information is required, a number of options are available. Hot wire anemometry and laser Doppler velocimetry require an open enclosure, altering the internal flow field. A third option is the use of liquid crystals to measure surface stresses present in the enclosure. While data from this method is limited to information on the surfaces of the disk, the drive can be run with its enclosure intact.

Shear-sensitive, temperature-insensitive liquid crystals are optically active esters of cholesterol and other sterol-related chemicals. They are composed of long helical molecules with a characteristic axial separation distance, as shown in Figure 4 below. When stresses are applied to these molecules, they relieve the additional strain energy either by coiling into tighter spirals or by partially uncoiling, depending on the direction of applied stress. This coiling or uncoiling behavior changes the characteristic axial separation between layers of the helix. The molecule acts as a diffraction grating, scattering incident white light into a spectrum determined by this spacing [Klosowicz, 1995]. Therefore, when viewed from a constant angle, the color seen by an observer will vary continuously, but non-linearly, as stress is increased. These effects are reversible for most liquid crystal mixtures within a compound-specific stress range, and the response times of the crystals used in this experiment are less than 1ms [Reda, 1993].

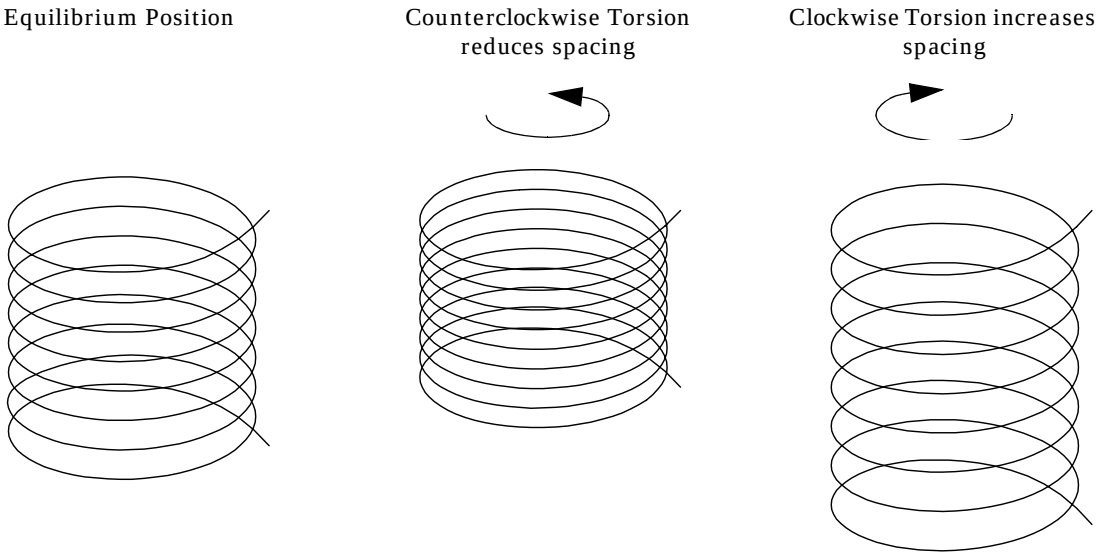

Figure 4: Coiling and uncoiling of a liquid crystal molecule under shear

The liquid crystals must be exposed to the flow in order to provide a measurement of surface shear stress. Therefore, they cannot be encapsulated like temperature-sensitive liquid crystals, but must be applied as an unsealed mixture of liquid crystals in solvent. As the solvent dries, the liquid crystals form a coating on the surface with no barrier between the crystals and the moving fluid. The solvent-crystal mixture is an extremely viscous liquid at room temperature and can be airbrushed onto surfaces of interest. A matte black background minimizes reflection and secondary scattering. Once the crystals are applied to a background, the hue shift of the crystals is measured from various angles while the disk is spinning. A plot of hue versus viewing angle for a single location on the surface reaches a maximum at some viewing angle. This maximum occurs when the camera and shear stress vector are aligned, giving the direction of the local stress vector. The value at the maximum is compared to a calibration curve, generated by measuring the response of a particular coating to the stress field in a known flow, to determine the magnitude of the shear stress at this point [Reda, 1996]. This process is repeated for all pixels in a captured image, and a vector plot of the shear stress field is constructed.

Shear stress data on the disk surface and the no-slip condition provide enough information to calculate the total drag on the spinning disk and a very accurate flow field near the disk surface. The accuracy of the flow field determined by this technique decreases with distance from the disk surface.

1.3.4 Rotating Reference Frame

A rotating reference frame considerably aids measurement of information from a high-speed rotating system. Since the disk can rotate through 90 revolutions per second and most cameras capture images at 30 Hz, the disk rotates through three full revolutions between frames. Fluid velocities in the tangential direction within the boundary layer above the disk are of the same order of magnitude as the purely tangential velocities found on the disk surface. If the camera is put into the same rotating frame of reference as the disk, the relative tangential components of velocity decrease in magnitude. This means that the relative magnitude of the velocity near the disk surface will decrease, allowing more accurate measurement of these velocities. It should be noted that the opposite is true outside of the boundary layer, where, by definition of the boundary layer thickness, tangential velocity is less than 1% of that of the rotating disk. In this case, the rotating reference frame would actually be detrimental to measurements, and a

fixed observation frame is needed. One way to capture information in a rotating reference frame is to rotate the camera at the same speed as the disk; however, it is nearly impossible to create a rotating electronic connection that is noise-free.

A better option is to mount the camera to a fixed surface, and rotate the image before it reaches the camera. We have manufactured a “rotoscope” in which a dove prism rotates instead of the camera. The technical details about the rotoscope and prism are discussed in section 2.2.

2 Setup

2.1 Drive Enclosure and Removable Media

The disk drive used in this experiment was the SyQuest 270, a 270 Mb removable hard drive system, provided by SyQuest Technology, Inc. Since the original drive was composed of opaque materials, the cover of the drive enclosure was replaced with clear plastic. The brown, translucent plastic top of the disk cartridge was also replaced with a transparent plastic cover of the same material and shape. These modifications made it possible to observe the surface of the disk without disturbing the flow field inside the drive enclosure or the disk cartridge. The power supply from an external SCSI enclosure powered the drive. Prior to the surface shear measurements, the drive's software was reprogrammed to allow operation irrespective of read/write errors; and a collision with the coated media necessitated the removal of the read/write head on the upper (observed) surface.

2.2 Optics

The recording system shown below in Figure 5 captured and recorded images of these experiments. All images passed through the dove prism, which was stationary during fixed frame observations. The prism reflected images about one of its axial planes, as shown in Figure 6. Any rotation of the prism through an angle θ resulted in the reflecting plane rotating through the same angle θ, so the image rotated through an angle 2θ, as in Figure 7. Not only could the camera remain fixed, but the prism's angular speed was reduced by a factor of two from that of the disk.

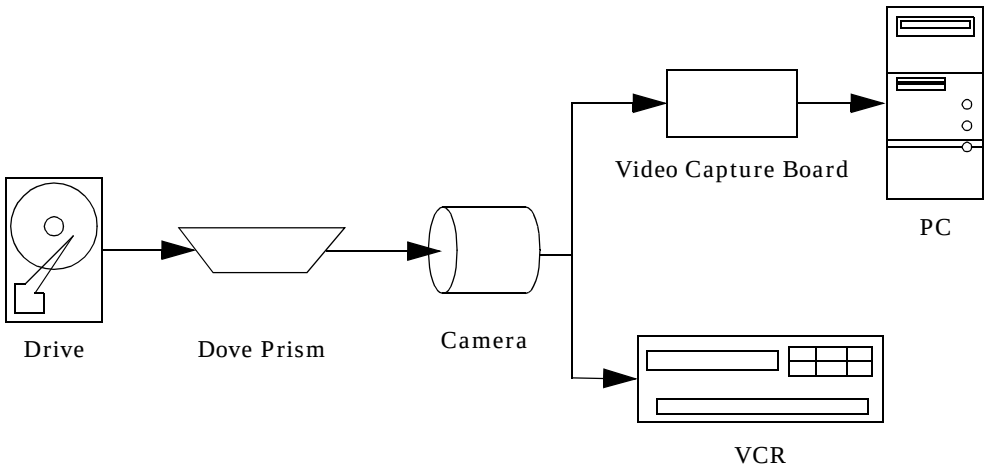

Figure 5: Diagram of Optics Setup

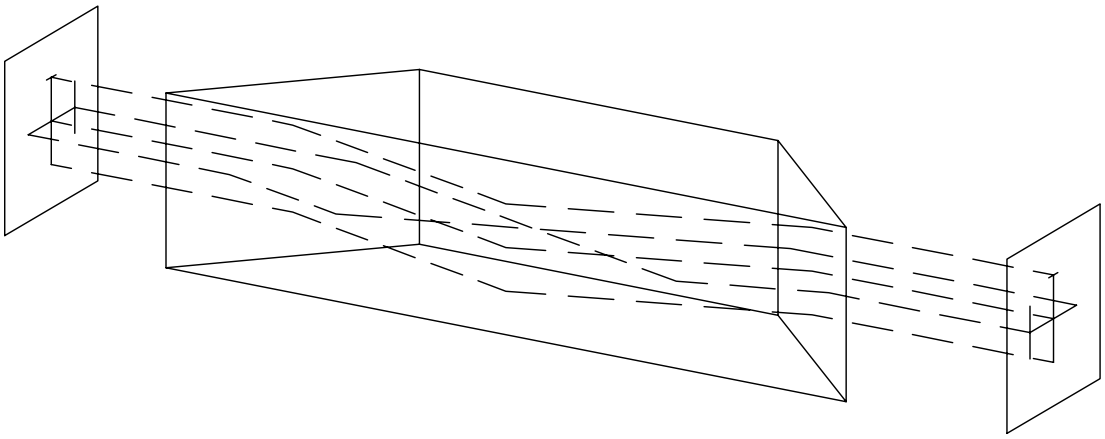

Figure 6: Reflection of an image through a dove prism

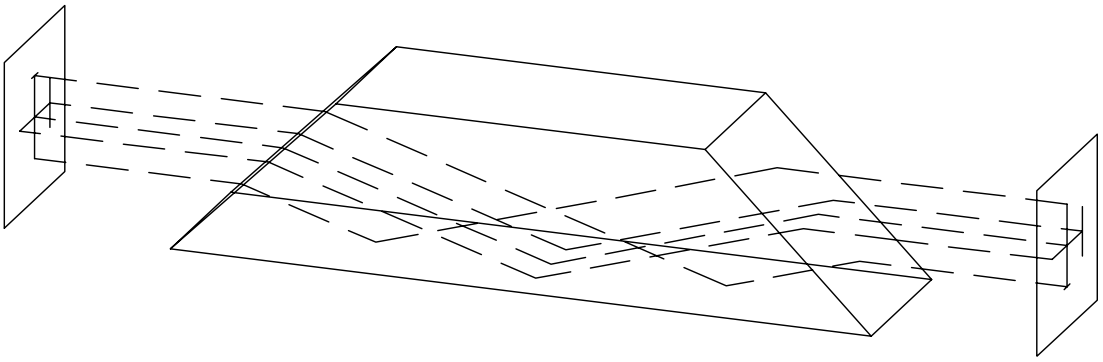

Figure 7: Rotation of the dove prism through a 90^{o} angle rotates the image through 180^{o}.

A rotoscope consisting of two cylinders that were free to rotate relative to one another housed the dove prism. During operation, the outer cylinder remained fixed, and was attached to the stator of a brushless motor, while the inner cylinder was free to rotate and was driven by the rotor of the brushless motor. Figure 8 is a schematic of the rotoscope. The dove prism was affixed to the inner cylinder after being aligned with the axis of both cylinders. The motor spun the inner cylinder at a speed that could be adjusted between about 200 and 3600 rpm. The speed was manually controlled, but remained nearly constant once initial adjustments had been made. The rotoscope provided the capability to record images for an extended period of time in a reference frame rotating from 400 to 7200 rpm.

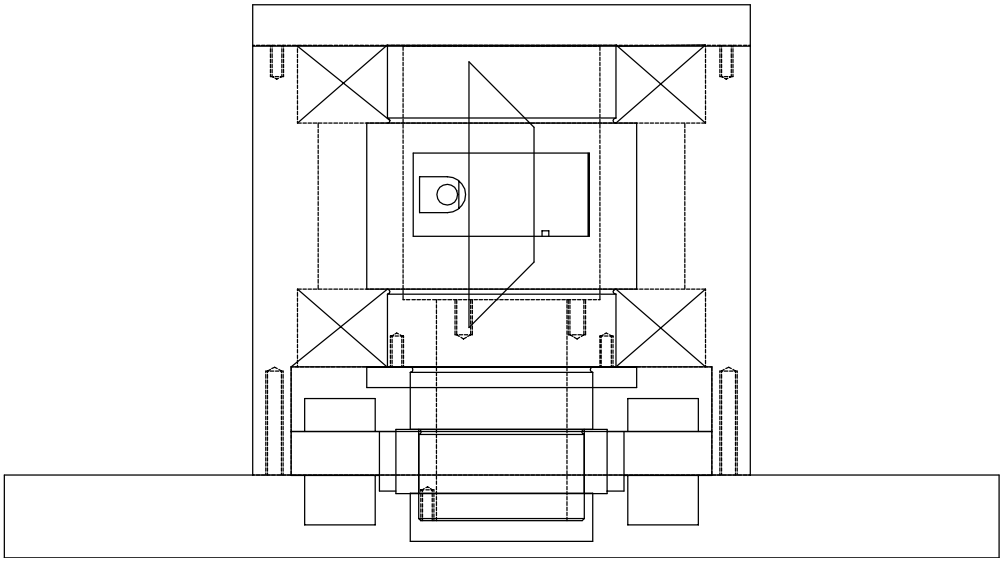

Figure 8: The Rotoscope

A Panasonic Color 3-CCD Camera (Model No. GP-US502) with a Canon 50mm lens transmitted the images to a Sony S-VHS Hi-Fi VCR (Model No. SVO-9500 MD). The resolution of the camera was 768 pixels in the horizontal direction by 494 pixels in the vertical direction. During flow visualization experiments, images were recorded under standard room lighting conditions. For all shear stress measurements, a single directional incandescent lamp illuminated the drive from an angle of 30 degrees above the horizontal plane. Images could be captured directly from the camera output on a Matrox Meteor RGB frame grabber with a resolution of 640 pixels by 480 pixels installed in a Pentium PC. Matrox Inspector v.1.71, a software package designed for the frame grabber, could then reduce the RGB data to a single hue component.

2.3 Flow Visualization

Two 1/8” holes drilled in the enclosure cover at radii of 0.125” and 1.25” from the center of the disk and two 1/8” holes drilled in the disk cartridge cover, aligned with the holes in the enclosure cover, permitted a qualitative analysis of the flow within the drive enclosure and disk cartridge. Using a custom-made delivery system with variable outlet pressure, frozen water vapor was introduced into the drive enclosure via these holes. During the tests, the drive read the magnetic media, and the reader arm alternated between two positions (Figures 9 and 10). When reading the disk, the head was positioned at its innermost position on the disk. Before loading the cartridge and after read/write errors occurred, the reader arm retracted to its default position outside of the disk cartridge.

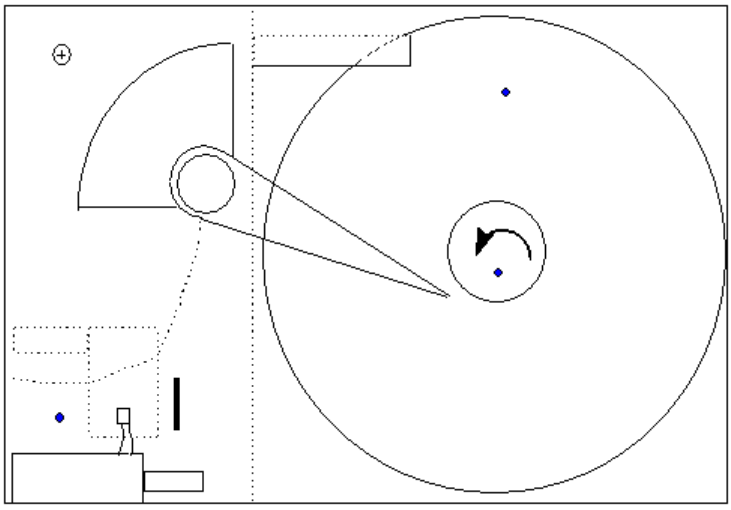

Figure 9: Schematic of the SyQuest 270 removable hard drive reading sectors near the center of the disk. The three dark circles indicate the points where vapor entered the drive.

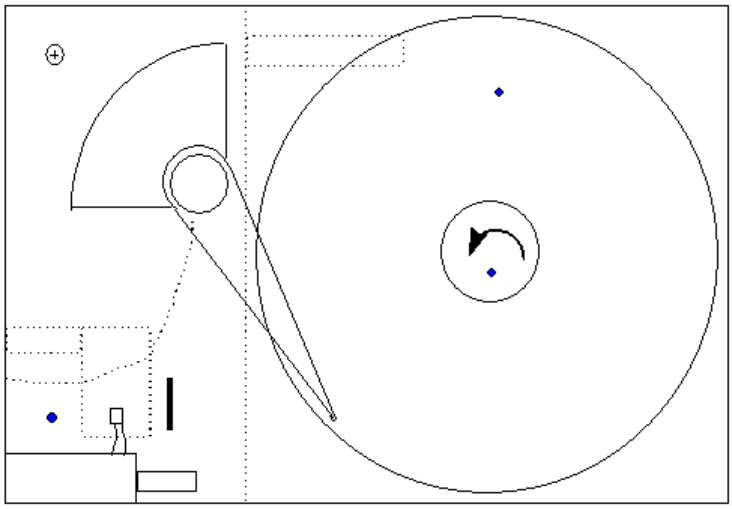

Figure 10: Schematic of the SyQuest 270 removable hard drive reading sectors near the outer edge of the disk. The three dark circles indicate the points where vapor entered the drive.

Sublimating dry ice (solid carbon dioxide) in warm water produced frozen vapor inside a container with two outlets. A variable clamp on one outlet regulated the vapor flow rate from the second outlet.

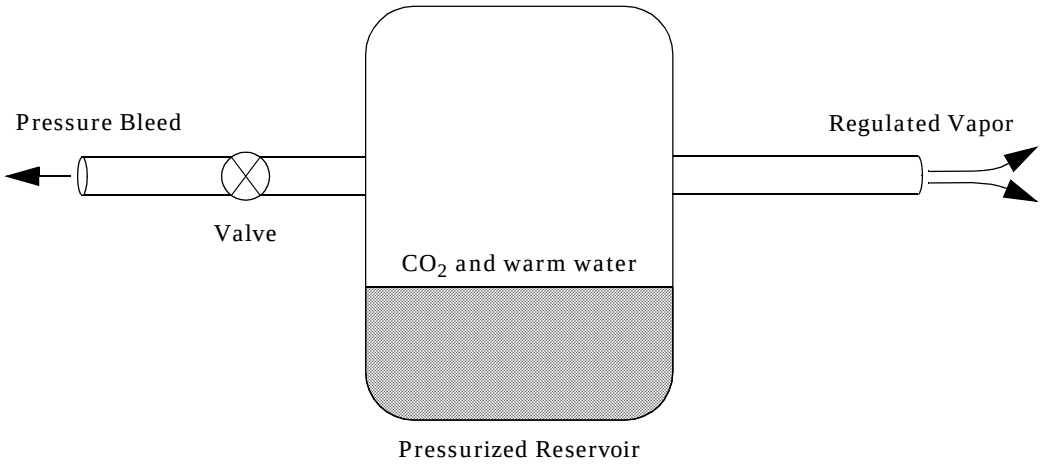

Figure 11: Water Vapor Production and Delivery System

2.4 Surface Stress Measurements

Using a Badger Model 350 Single Action External Mix Air-Brush and compressed air, a uniform layer of matte black background paint (Hallcrest BB-G1) was applied to the upper surface of the media. After the black paint had dried, a liquid crystal coating was sprayed onto the same surface of the disk. The combined thickness of the two layers measured between 25 and 50 μm, with the background paint composing all but 5 to 10 μm of this thickness.

Two different liquid crystal suspensions were used in the initial tests of this process: Hallcrest BCN/192 and Hallcrest CN/R3. These mixtures differed in two important ways: their viscosities and their stress measurement ranges. According to product information from Hallcrest, the CN/R3 is roughly four times more viscous than the BCN/192 mixture. Centrifugal accelerations of up to 1500 g at the outer edge of the disk present due to the high speed rotation of the disk made the viscosity difference significant.

After coating the disk with each of the crystal mixtures, the disk spun at its normal operating speed with the reader arm fixed at a position near the center of the drive. Observations were made in both a fixed frame and rotating frame.

3 Results

3.1 Flow Visualization

Frozen water vapor particles were introduced into the drive from three points. The data taken in a fixed reference frame from each of these locations revealed a portion of the flow field near their respective insertion points. Due to the rapid dissipation of the fog upon returning to room temperature, fog particles generally traveled less than one revolution before condensing. Information from the three regions was pieced together to generate a representation of the flow field, shown in Figures 12 and 13, in each of the two relevant reader arm positions.

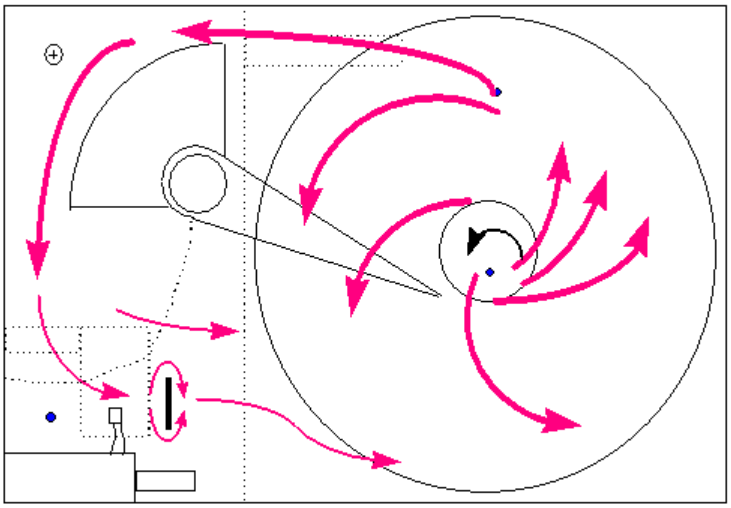

Figure 12: Arrows indicate local flow direction when reader arm is in the inner position. Thicker arrows represent higher velocities.

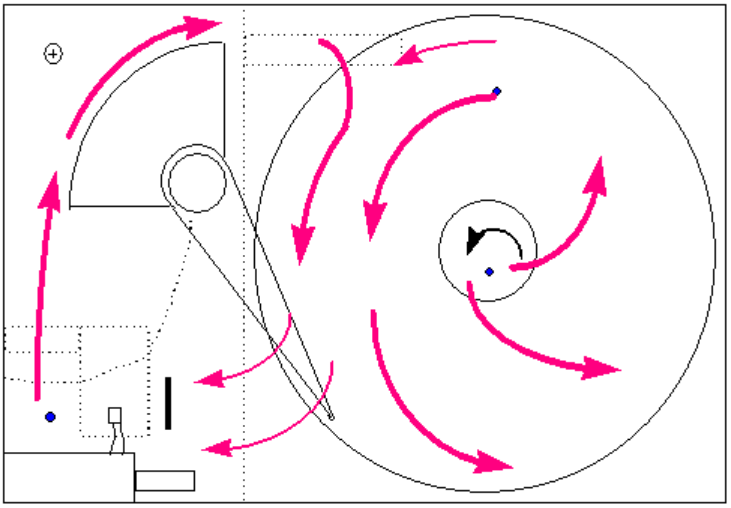

Figure 13: Arrows indicate local flow direction when reader arm is in the outer position. Thicker arrows represent higher velocities.

The air near the disk surface flowed outward and counterclockwise (in the direction of disk rotation) over the entire disk surface. In the regions close to the reader arm, where the flow was not constrained by a side wall, the flow differed for various reader arm positions. When the reader arm was close to the disk's center, fluid moved from the cartridge area into the armature area on the side of the drive away from the reader arm (see Figure 12 above), while fluid returned to the cartridge area on the reader arm side (see Figure 13 above). In contrast, when the arm was nearer the edge of the platter, the fog traveled in the opposite direction in the armature area. Another feature of the flow is the behavior of air near the filter installed to remove contaminants from the drive. Upon encountering the filter, the water vapor particles split into two streams that rejoined behind the filter, similar to the behavior seen when a flat plate is inserted into a flow perpendicular to the flow direction. In addition to the three locations used to determine the internal flow field, fog was introduced near the front of the drive. The front of the drive enclosure did not entrain fluid during disk operation.

Flow visualization revealed the basic qualitative details predicted by incompressible theory. A cell structure formed within the enclosure after initial start-up transients decayed. Although the cell structure varied with reader arm position, a well-defined flow circuit was evident in both cases. While filtration of the air inside the drive is critical to dust reduction, the ratio of the flow rate of air through the filter to the total circuit flow rate in the enclosure is small. The filter can be compared to a large resistor in an electric circuit. If electricity can find a lower resistance path, most of the current flow will use it. The lower resistance path in this case is to circumvent the filter like an obstacle in the flow path. While this requires more energy than following a straight flow path, it requires less energy than passing through the small, high viscosity channels of the filter material. The front of the drive did not entrain fluid into the drive enclosure, indicating that a majority of contaminants within the drive must enter when the cartridge is inserted into the drive, attached to the outside of the cartridge surface.

3.2 Liquid Crystals

The BCN/192 liquid crystals on the surface of the disk had a mottled, nonuniform appearance with a reddish-brown hue prior to operation of the drive. While the disk accelerated to 5400 rpm, the color of the liquid crystal mixture shifted to a greenish hue. Although the entire surface appeared to shift, it was difficult to resolve any spatial variation in the color change, except for two brighter sectors of about 30 degrees opposite one another. These sectors remained at fixed locations except that they rotated around the disk when the single incandescent lamp used to light the experiment was moved around the disk. When the disk slowed to a stop, the color shift reversed, and the liquid crystals returned to their original reddish-brown hue. Examination of the liquid crystal coating after running the disk at full speed revealed a radial pattern on the disk surface, as well as an accumulation of liquid crystal droplets on the interior of the disk cartridge. At the radius where the read/write head was positioned over the disk, the liquid crystal mixture had been stripped away from the disk surface, but the black background paint remained intact. During this stage of the experiment, the upper read/write head was rendered inoperative.

After removal of the now-defunct read/write head, the more viscous CN/R3 liquid crystal mixture was tested in a similar manner. The color of the liquid crystal mixture ranged from a greenish-yellow hue prior to rotation to a bluish hue while rotating at full speed. A radial streaking pattern was observed in the liquid crystals after the experiment and some droplets were found on the inside surface of the disk cartridge, although there was less mass transfer than in the case of the less viscous BCN/192 mixture. Although the read/write head had been removed, the reader arm still contacted the liquid crystal layer, removing a band of liquid crystals from the disk surface.

When the CN/R3-coated rotating disk was viewed in the rotating frame, the image appeared to be steady. Approximately one half of the disk was a reddish-orange hue, while the other half was much closer to blue-green. This color pattern appeared to be steady in the rotating frame of reference.

Liquid crystal results indicate that shear stresses increase with angular velocity over the entire disk surface, but the expected linear increase in shear stress with radius is not evident. The two liquid crystal compounds responded with different color play responses. Neither mixture reached a clearing point (stress that exceeds the maximum measurable stress of the compound), so either is usable for shear stress measurements. Hue gradients over the disk surface were not visible by eye, except for the two steady regions in the fixed frame. These regions were due to the lighting used for the experiment. The behavior in the rotating frame should not be steady, so interpretation of the rotating frame images recorded in this experiment is difficult without further investigation of the effects of lighting on the liquid crystals.

4 Conclusions

4.1 Progress

Flow visualization generated a flow field that validated the comparison to the infinite disk problem. While there are details of the flow that differ from this problem, the causes of the differences are evident. Liquid crystal application and testing raised new questions about the forces at work within the drive enclosure, especially near the disk surface. While quantitative results were not realized, understanding of the effects of shear stress and lighting on the liquid crystal coatings improved. Subsequent testing will establish a quantitative velocity field inside the disk enclosure.

4.2 Problems

The greatest obstacle to constructing a full flow field is an analysis of the effects of centrifugal forces on the liquid crystal coatings. As noted previously, a particle following a circular path of less than 5 cm at an angular speed of 5400 rpm experiences an acceleration of up to 1500g. The liquid crystals are applied as an unsealed mixture, anchored to the disk only by friction. An outward radial flow is generated in the liquid crystal layer, as evidenced by the radial streaking pattern found on the platter surface after high speed testing. This radial flow contains stress gradients similar to those found in other free surface flows. Since the density of the liquid crystal coating is much greater than that of air, the shear stress supported by the free surface will be much smaller in magnitude than the shear stresses present within the layer. Therefore, liquid crystals at different depths in the layer may experience different stresses, and the observed color shift may vary with depth. A number of factors other than shear stress influence the color shifting of the liquid crystals, including lighting, layer depth, observation angle, and centrifugal forces. More observations of these effects are required for an accurate analysis of their effects on the crystals.

The effects of the read/write head could not be observed during the liquid crystal tests, due to the contact between the head and the liquid crystal layer. The background paint forms a layer 25 to 50 microns thick. Elimination of this layer without loss of color play effects would be beneficial to further data collection.

The speed of events within the drive requires faster image acquisition. It is possible that there are fluctuations occurring more rapidly than the camera can record. Currently, images are captured at a rate of 30 Hz. Flash lamps will increase the effective shutter speed of the video equipment. Images in the rotating frame of reference will experience less smearing, and distinct locations will be more easily analyzed.

4.3 Future Directions

As an overall system for the analysis of hard drive systems, these techniques appear to be effective, although further tests of their capabilities and limitations will be necessary to maximize their efficiency and accuracy. In order to develop quantitative information from the liquid crystal data, the effects of centrifugal forces on the liquid crystal layer must be understood. Digital particle image velocimetry (DPIV) would allow calculation of velocity fields directly from the motion of particles in the drive. This technique has been very successful in lower speed flows. Regions of slower flow could be observed directly in the fixed frame, while the higher speed regions of the flow nearer to the platter surface could be examined using the rotoscope. Further development of liquid crystal technology and particle image velocimetry will allow the construction of more quantitatively detailed flow fields.

4.4 Summary

During the past year, significant progress has been made toward universal analysis of the fluid flow phenomena within a disk drive. Flow visualization provided a detailed but qualitative

analysis of flow within the drive under various operating conditions. Liquid crystal measurement techniques were developed based on similar techniques used in aerospace applications. To aid in these measurements, a rotoscope was constructed to provide a reference frame that rotated with the disk surface. Extrapolation techniques for the analysis of the resulting shear stress data have been developed and await further data to allow construction of the velocity field within the drive. Particle image velocimetry can then be used to confirm these results. All of the analytical methods used in these experiments are universally applicable to disk drives with proper adaptations (replacement of opaque surfaces with clear counterparts).

To design drive enclosures based on the global flow field within the drive, simple flow visualization, analytical results, and order of magnitude estimates should be sufficient.

References:

Bouchez, J. P. and Goldstein, R. J. (1975), Impingement cooling from a circular jet in a cross flow, *Int. J.Heat Mass Transfer* **18**, 719-730.

Karman, T. von (1921), Uber laminare und turbulente Reibung, *Z. Angew. Math. Mech.* **1**, 233-252 (English translation in NACA Technical Memo. 1092).

Klosowicz, S. J. and Zmija, J. (1995), Optics and Electro-optics of Polymer-dispersed Liquid Crystals: Physics, Technology, and Application, *Optical Engineering 34(12) (December 1995)*, 3440-3450.

Konwerska-Hrabowska, J. (1995), Precise Optical Force Sensors made of Polycarbonate or Epoxyde Disks *Optical Engineering 34(12) (December 1995)*, 3433-3439.

Merzkirch, W. (1987), *Flow Visualization*, Academic, Orlando, FL.

Panton, R. L. (1984), *Incompressible Flow*, Wiley, New York.

Reda, et. al. (1996), Areal Measurements of Surface Shear Stress Vector Distributions Using Liquid Crystal Coatings, AIAA 96-0420.

Reda, et. al. (1993), Experimental Investigations of the Time and Flow-Direction Responses of Shear-Stress-Sensitive Liquid Crystal Coatings, AIAA 93-0181.

White, F. M. (1991), *Viscous Fluid Flow*, McGraw-Hill, New York.

Wolna, M. (1995), Polymer Materials in Practical Uses of Photoelasticity, *Optical Engineering 34(12) (December 1995)*, 3427-3432.